*Corresponding Author Email: abatchal@yahoo.fr

Proceedings of the World Conference on Research in Teaching and Education

Vol. 2, Issue. 1, 2023, pp. 24-34

DOI: https://doi.org/10.33422/worldte.v2i1.58

Copyright © 2023 Author(s) ISSN: 2783-7750 online





Impact of Power-Line Communication Radiation on Human Health

Abba K L Abatcha*, Abdourahimoun Daouda and Makinta Boukar

Ph.D., Physics Department, Abdou Moumouni University of Niamey, Niger Republic

Abstract

The advent of smart electrical grids (Smart-grids) has created the need for a reliable communication system within traditional electrical grids. Many technologies are available on the market for communication in smart-grids environment. Communication using PLC (Power-Line Communication or power-line carrier) technology is by far the best choice for operators of these smart-grids, because it uses the electrical cables already in place as a communication link. Unfortunately, since the electrical grid (frequency = 50/60 Hz) was not designed for the transport of high-frequency signals, in PLC mode (100 kHz - 30 MHz) the electrical cables behave like antennas and emit electromagnetic radiation in the nearby environment. This work is a contribution in the evaluation of electromagnetic radiation impact of PLC technology on human health. According to ICNIRP (International Commission for Non-Ionizing Radiation Protection), this type of assessment in done base on SAR (Specific Absorption Rate) and ΔT (tissue temperature raising during exposure to radiation). PLC cables radiation SAR and ΔT are confront with ICNIRP-limits (Guidelines). In order to cover many exposure scenario, interaction between the radiation of an Outdoor-PLC cable and a human head have been analyze using analytical approach (Maxwell equations) and numerical approach (simulation with Feko software). These analyses have demonstrated that exposure to Outdoor-PLC cable electromagnetic radiation is not harmful to human being. For a long-term exposure of human head to PLC cable electromagnetic radiation, The SAR is less than 1nW/Kg and ΔT under 10⁻⁵ °C (Far from ICNIRP limits). Analyses have also produce a simplified expression of PLC cable electromagnetic radiation SAR base on Biot-&-Savart law.

Keywords: smart-grids, Power Line Communication, electromagnetic radiation, Specific Absorption Rate

1. Introduction

PLC (Power-Line Communication or power-line carrier) technology is a communication system that uses electrical cables/wires as information (data) carriers. Electrical cables are design for the transport of low frequency electrical signal (50 or 60 Hz). When high frequency signal (PLC signal) is injected in these electrical cables, they react like antennas by radiating in the nearby environment. Although emitting parasitic electromagnetic radiation, PLC technology brings an undeniable advantage to smart-grids operators: save of money, security and simplicity of implementation.

Regarding the fast deployment of PLC technology nowadays, it is necessary to evaluate the impact of its electromagnetic radiation on the neighboring environment. Several epidemiological and experimental studies have been conducted on this subject and most of them have led to the establishment of biological effects that could threaten human health (Abatcha et al., 2023; KONLACK & TCHUIDJAN, 2011; Park, 2023; Vaverka et al., 2023).

Since PLC radiation is non-ionizing radiation, its biocompatibility (environmental friendship) is regulate by the guideline of ICNIRP (International Commission for Non-Ionizing Radiation Protection). ICNIRP establishes the limits of exposure to radiation in the PLC band (100 kHz - 30 MHz) through the SAR (Specific Absorption Rate) ("Determining the Peak Spatial-Average Specific Absorption Rate (SAR) in the Human Body from Wireless Communications Devices, 30 MHz to 6 GHz - Part 3," 2017; International Commission on Non-Ionizing Radiation Protection, 2022).

To assess the SAR or the amount of energy absorbed by the tissues, most systems measure either the internal electric fields (E_i) or the temperature increases in these tissues (ΔT). In practice, determining the E_i or the ΔT is tedious, hence the use of numerical solutions (Altair-Feko software).

In this work, we will firstly seek the analytical expression of the electric fields knowing the distribution of the current through the electric cables and the analytic expression of the SAR. Secondly, we will use these analytical expressions to analyze the impact of PLC radiation on human health.

2. Analytic expressions

When a human entity is exposed to electromagnetic radiation, the amount of energy absorbed by the tissues is defined by SAR as in Eq. 1 and 2 (International Commission on Non-Ionizing Radiation Protection, 2022; Zagar et al., 2023):

$$SAR = \gamma. (|E_i|^2/\rho)$$
 (1)

$$= C_i. (\Delta T/\Delta t)$$
 (2)

Where:

Ei: Internal electric field in the tissue [V/m]

ρ: Density of the tissue [kg/m3];

γ: Electrical conductivity of the tissue [S/m];

Ci: Heat capacity of the tissue [J/kg/°C];

 Δt : Exposure time [s];

 ΔT : Temperature rise during exposure time [°C].

Electromagnetic radiation is composed of the electric field (↑E) and the magnetic field (↑H). The expressions of these two fields are governed by Maxwell's four equations (Eq. 3 to 6) (Alihodzic et al., 2022; Frère, 2017):

$$div \uparrow D = \rho \tag{3}$$

$$\uparrow rot \uparrow E = - (\partial \uparrow B / \partial t) \tag{4}$$

$$div \uparrow B = 0 \tag{5}$$

$$\uparrow \text{rot} \uparrow H = - (\partial \uparrow D / \partial t) + \uparrow j \tag{6}$$

With Eq. 7 to 10 ((PDF) Analysis of Variational Formulations and Low-Regularity Solutions for Time-Harmonic Electromagnetic Problems in Complex Anisotropic Media, n.d.; Peng et al., 2020):

$$\operatorname{div}\uparrow \mathbf{j} + \partial \rho/\partial \mathbf{t} = 0 \tag{7}$$

$$D = \boldsymbol{\varepsilon}.E = \boldsymbol{\varepsilon}_0.\boldsymbol{\varepsilon}_r. E \tag{8}$$

$$B = \mu . H = \mu_0 . \mu_r . H$$
 (9)

$$Z = E/H = \sqrt{(\mu/\epsilon)}$$
 (10)

where

D: Electric Induction

B: Magnetic Induction

E: Electric Field

H: Magnetic Field

J: Current Density

ρ: Density

 $\varepsilon_r / \varepsilon_0$: Relative Permittivity / Vacuum Permittivity

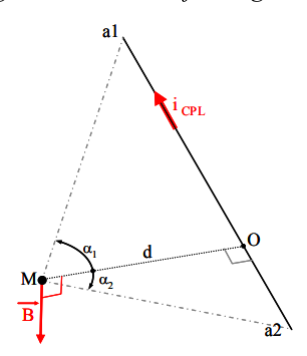
 μ_r/μ_0 : Relative Permeability / Vacuum Permeability

Z: Characteristic impedance of the medium

In the case of a power line (Figure 1) traversed by a PLC signal (i_{plc}), the magnetic induction †B at point M is given by the law of <u>Biot and Savart</u> in Eq. 11 (CALCUL DU CHAMP MAGNÉTIQUE RAYONNÉ PAR DEUX FILS RECTILIGNES PARALLÈLES PARCOURUS PAR UN COURANT ELECTRIQUE, n.d.; Peng et al., 2020; Poljak et al., 2019):

$$\|\uparrow \mathbf{B}_{2\text{wires}}\| = [(\mu_0.\mathbf{I}_{\text{cpl}})/(4.\pi.\mathbf{d}_+)]^*[\sin(\alpha_2) - \sin(\alpha_1)]$$
(11)

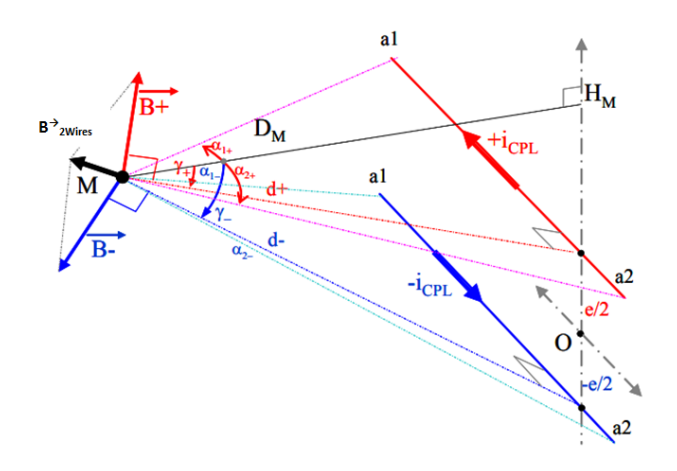
Figure 1: Magnetic induction of a single-wire PLC cable



Base of the expression of the magnetic induction radiated by a single-wire-cable (Eq. 11) at a distance d (Figure 1), we will calculate at the point M (Figure 2) the magnetic inductions (\uparrow B) radiated by a two-wire-cable. In this case (two-wire-cable), vector \uparrow B is a sum of \uparrow B+ (radiation emitted by forward current in the phase wire) and \uparrow B- (radiation emitted by reverse current in the neutral wire).

$$\uparrow B_{2wires} = \uparrow B_+ + \uparrow B_-$$

Figure 2: Magnetic induction of a two-wire power-line cable



From Eq. 11, we generate Eq. 12 and 13:

$$\uparrow B_{+} = [(\mu_{0}.I_{cpl})/(4.\pi.d_{+})] * [\sin(\alpha_{2+}) - \sin(\alpha_{1+})] * \uparrow u_{+}$$
(12)

$$\uparrow B- = [(\mu_0.I_{cpl})/(4.\pi.d-)] * [\sin(\alpha_2-) - \sin(\alpha_1-)] * \uparrow u-$$
(13)

When the point M belongs to the line perpendicular to the segment [a₁, a₂] and passing through its center (Figure 3), we have:

$$\alpha_{1+} = \alpha_{1-} = -\alpha_{2+} = -\alpha_{2-} = \alpha$$
 & $\uparrow u_{+} = -\uparrow u_{-} = \uparrow u_{-}$

Figure 3: Above hypothesis illustration

neutral phase

$$\uparrow B_{+} = + \left[(\mu_0.I_{cpl})/(2.\pi.d) \right] * \sin(\alpha) * \uparrow u$$
 (14)

$$\uparrow B_{-} = - \left[(\mu_0.I_{cpl})/(2.\pi.(d+r)) \right] * \sin(\alpha) * \uparrow u$$
 (15)

$$\uparrow B_{2wires} = [(\mu_0.I_{cpl})/(2.\pi)] * [r/(d.(d+r))] * \sin(\alpha) * \uparrow u$$

Taking the case where $r \ll d$,

$$\uparrow B_{2\text{wires}} = [(\mu_0.I_{\text{cpl}}.r)/(2.\pi.d^2)] * \sin(\alpha) * \uparrow u$$

In the case of a very long wire (infinite wire) the angle α tending towards to $\pi/2$ therefore:

$$\uparrow B_{2\text{wires}} = [(\mu_0.I_{\text{cpl}}.r)/(2.\pi.d^2)] \uparrow u$$

$$B = \|\uparrow B_{2\text{wires}}\| \Rightarrow$$

$$B = (\mu_0.I_{\text{cpl}}.r)/(2.\pi.d^2)$$
(16)

At point M, the magnetic induction generates a magnetic field H₀ given by Eq. 9:

$$B = \mu_0 . \mu_r . H$$

As we still in a vacuum, μ_r = 1 therefore:

$$H_0 = \beta / \mu_0 \tag{17}$$

with $\mu_0 = 4.\pi \cdot 10^{-7} (H/m)$.

Eq. 10 and 16 gives us the expression for the electric field E₀ radiated by the two-wire-cable.

$$E_0 = H_0.Z_0 (18)$$

with
$$Z_0 = \sqrt{(\epsilon_0/\mu_0)} = 377~\Omega$$
 as $\epsilon_0 = 8.854.10^{-12} (F/m)$ and $\mu_0 = 4.\pi.10^{-7} (H/m)$.

Exposure of the head to the E₀ field creates electrical-charges movement on its surface. This phenomenon generates an opposing electric field E' such that (*CALCUL DU CHAMP MAGNÉTIQUE RAYONNÉ PAR DEUX FILS RECTILIGNES PARALLÈLES PARCOURUS PAR UN COURANT ELECTRIQUE*, n.d.; *Effect of Electromagnetic Waves on Human Reproduction - PubMed*, n.d.; Pola, 2023):

$$E' = \sigma/\epsilon_0$$
 σ : surface charge density

So the electric field that is actually applied to the head is E_a with (CALCUL DU CHAMP MAGNÉTIQUE RAYONNÉ PAR DEUX FILS RECTILIGNES PARALLÈLES PARCOURUS PAR UN COURANT ELECTRIQUE, n.d.; ICNIRP | Publications, n.d.):

$$E_a = E_0 - E'$$
 (19)

The field E_a applied to the head creates inside it an induced field E_i such that (CALCUL DU CHAMP MAGNÉTIQUE RAYONNÉ PAR DEUX FILS RECTILIGNES PARALLÈLES PARCOURUS PAR UN COURANT ELECTRIQUE, n.d.; ICNIRP | Publications, n.d.):

$$Ei = (1/\boldsymbol{\varepsilon}_{r}). Ea$$

$$= (1/\boldsymbol{\varepsilon}_{r}). (E_{0}-E')$$

$$= (1/\boldsymbol{\varepsilon}_{r}). [E_{0}-(\gamma/\boldsymbol{\varepsilon}_{r})]$$
(20)

However the creation of the induced field E_i by E_a is accompanied by the creation of an induced current of density J (*CALCUL DU CHAMP MAGNÉTIQUE RAYONNÉ PAR DEUX FILS RECTILIGNES PARALLÈLES PARCOURUS PAR UN COURANT ELECTRIQUE*, n.d.; *ICNIRP* | *Publications*, n.d.):

$$J = \sigma$$
. E_i (21)

with

$$J = d\sigma/dt$$

 $J = j.\omega.\sigma$ (in alternative regime $\omega=2.\pi.f$).

therefore, Eq. 20 becomes (CALCUL DU CHAMP MAGNÉTIQUE RAYONNÉ PAR DEUX FILS RECTILIGNES PARALLÈLES PARCOURUS PAR UN COURANT ELECTRIQUE, n.d.; ICNIRP | Publications, n.d.):

$$E_i = [E_0/\varepsilon_r \cdot (1/(1+(\sigma/(j.\omega.\varepsilon_r))))]$$
(22)

By replacing the term E_i by its expression from Eq. 22 in Eq. 1 we will have (CALCUL DU CHAMP MAGNÉTIQUE RAYONNÉ PAR DEUX FILS RECTILIGNES PARALLÈLES PARCOURUS PAR UN COURANT ELECTRIQUE, n.d.; ICNIRP | Publications, n.d.):

If
$$[\sigma/(j, \omega, \varepsilon_0, \varepsilon_r)] \ll 1$$
 then $E_i = E_0/\varepsilon_r \Rightarrow$ insulating body

If
$$[\sigma/(j, \omega, \varepsilon_0, \varepsilon_r)] \gg 1$$
 then $E_i = E_0$. $[(j, \omega, \varepsilon_0)/\sigma] \Rightarrow \text{conductive body}$ (23)

By replacing the term E_i by its expression from Eq. 23 in Eq. 1 we will have:

SAR =
$$[\sigma. |E_0.((j.\omega.\epsilon_0)/\sigma)|^2]/\rho$$

= $|E_0.j.\omega.\epsilon_0|^2/(\rho.\sigma)$

By integrating Eq. 16, 17 and 18 into the expression above, we will have:

SAR =
$$|(j.\omega.\epsilon_0.Z_0.I_{cpl}.r)/(2.\pi.d^2)|^2/(\rho.\gamma)$$

SAR = $\beta.I_{cpl}^2$ (24)
with $\beta = |j.(Z_0.f.r.\epsilon_0)/d^2|^2/(\rho.\gamma)$

By replacing the SAR expression of Eq. 24 in Eq. 2, we will have:

$$\beta.I^{2}_{cpl} = C_{i}.\Delta T/\Delta t \Rightarrow \Delta T = \beta.I^{2}_{cpl}.\Delta t/C_{i}$$
(25)

3. Radiation analysis and evaluation

3.1 Methods

The impact assessment of non-ionization radiation such that of PLC technology is governed by the guideline of CNIRP. ICNIRP assess radiation of PLC-band (0.1-30 MHz) with SAR and ΔT . As it is tedious to measure the real SAR or ΔT , we will first simulate a PLC communication in order to get the current distribution in electrical wires (numeric approach). The current distribution will help us to generate the SAR and ΔT base of analytical expressions established in Eq. 24 and 25 (analytic approach).

By confronting this two data (SAR & ΔT) with ICNIRP limits, we can appreciate the impact of PLC radiation on human being.

The simulation of current distribution will be along a 200 meters aluminum cable traversed by an alternating current of variable frequency (0.1-30MHz). This simulation is done on Feko software. Feko is a high scale tool for the analysis of electromagnetic radiation by the method of moments (MOM). Feko will also simulate and help to analyze the exposure of a human head (10cm radius sphere filled with cerebrospinal fluid) to radiation from the cable.

3.2 Results and discussion

The current distribution is a function of frequency and the distance from the power source. Figure 4 illustrates the current distribution along the cable for four different frequencies (f_1, f_2, f_3, f_4) .

The shape of the distributed current is proportional to the injected current wavelength. Its ranges from a rising edge for the frequency $f_1(0.1\text{MHz})$ to a sinusoid for $f_4(30\text{MHz})$ passing through more spread sinusoids for $f_2(1\text{MHz})$ and $f_3(10\text{MHz})$.

The amplitude of the four injected signals are identic. The variation of the amplitude of distributed signals along the cable is due to the combination of two parasitic effects:

- the skin effect, which forces the current to flow towards the surface of the conductor;
- the proximity effect which creates a kind of attraction between the current of the phase conductor (I_{cpl+}) and that of the neutral conductor (I_{cpl-}).

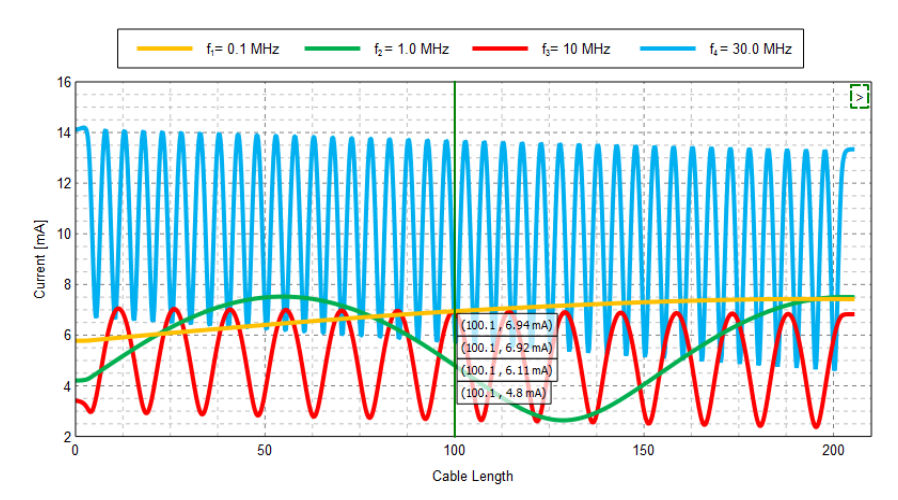


Figure 4: Current Distribution

By centering the observation of distributed current on a specific point of the cable, amplitude behavior is clearer. Figure 5 summarizes this current distribution in the center of the cable as a function of PLC frequencies. The attenuation of the signal between point A and B of more than 50% illustrates the loss of energy as the frequency of the signal increases. This loss of energy is responsible for the electromagnetic radiation of the conductors.

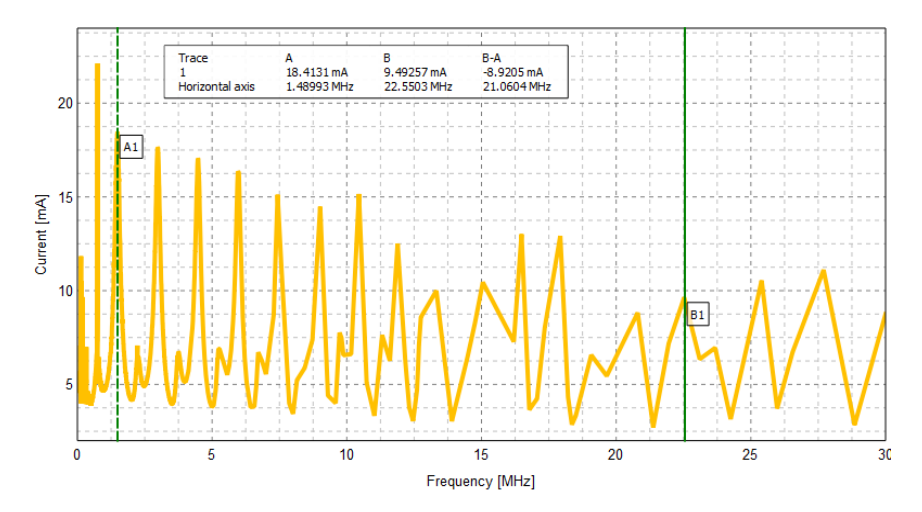


Figure 5: PLC current distribution (Icpl) as a function of frequencies in the middle of the cable

Using the current distribution at the center of the cable and Eq. 16 to 18, we calculate the electric field (E-field) around point M (inside the dummy head). On Figure 6 by superimposing calculated E-field and generated E-field (from Feko), we observe that many points converge except for a few peak points in the 100kHz-to-7MHz band. These few points of non-convergence are due to the significant difference in the sampling steps of the field to be calculated compared to the generated field.

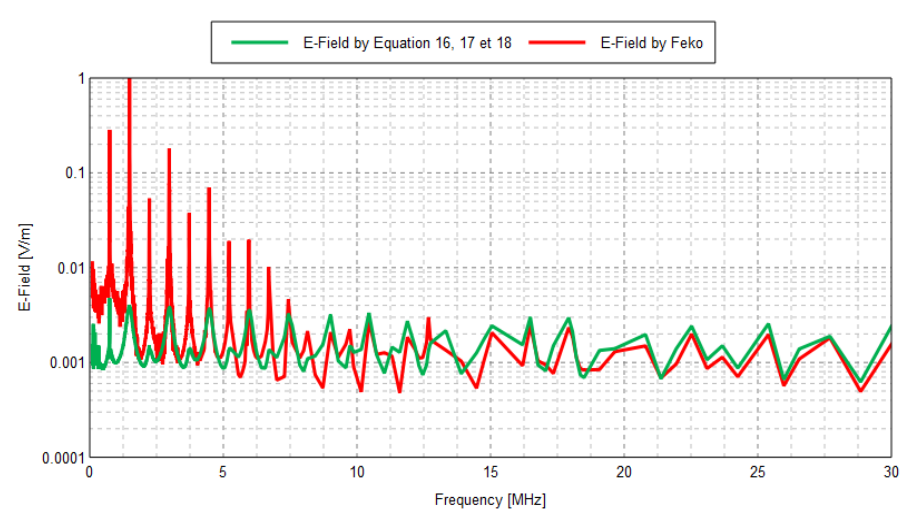


Figure 6: Field E0 at point M

Knowing the electric field at point M, the SAR inside the human head (dummy) is calculated with Eq. 24. The Figure 7 is a representation of the calculated SAR and that

generated by Feko. With the exception of the 100kHz-to-7MHz band where the SAR generated is influenced by the peaks of the electric field, the two curves are similar.

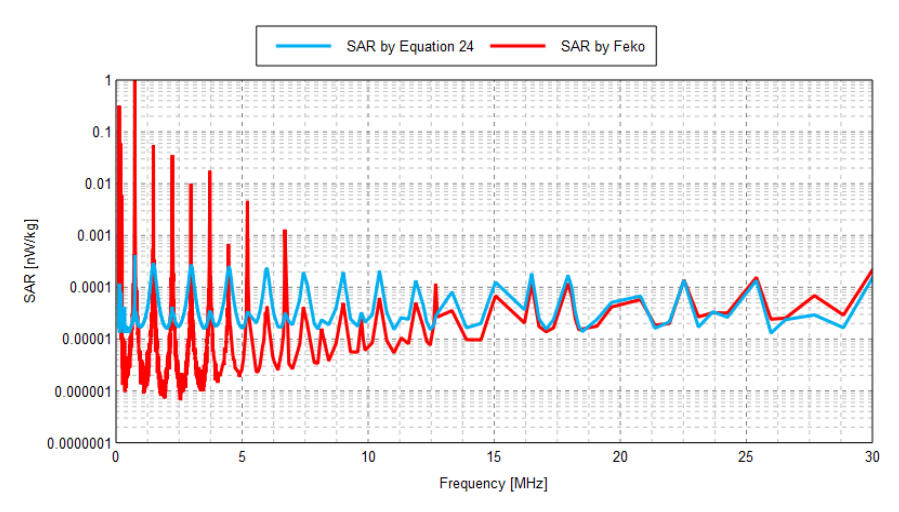


Figure 7: Specific Absorption Rate (SAR)

ICNIRP has set the SAR limit at 2W/kg at head level (International Commission on Non-Ionizing Radiation Protection, 2022; Park, 2023; Razek, 2023) but the calculated SAR (Figure 8) does not exceed one nanowatt per kilogram(1nW/Kg) well below the threshold. As this limit (ICNIRP) is based on an exposure of approximately 6 minutes, we can conclude that PLC radiation is not harmful for a short-term exposure.

For exposures of longer duration, the determination of the increase in tissue temperature is the best indicator of the impact of radiation on human health. According to ICNIRP, any rise in temperature above 2° C that the body cannot compensate for, can have harmful effects such as heatstroke or sunstroke. Studies conducted on animals and cellular systems have revealed several health disorders for a rise in body temperature of 1 to 2° C and varying durations of exposure (Askari et al., 2023; Frère, 2017). The temperature rise in the dummy's head is evaluated using equation 25. This increase in tissue temperature (Δ T) is illustrated in Figure 9 for exposure times (Δ t) ranging from 30 minutes to a whole day.

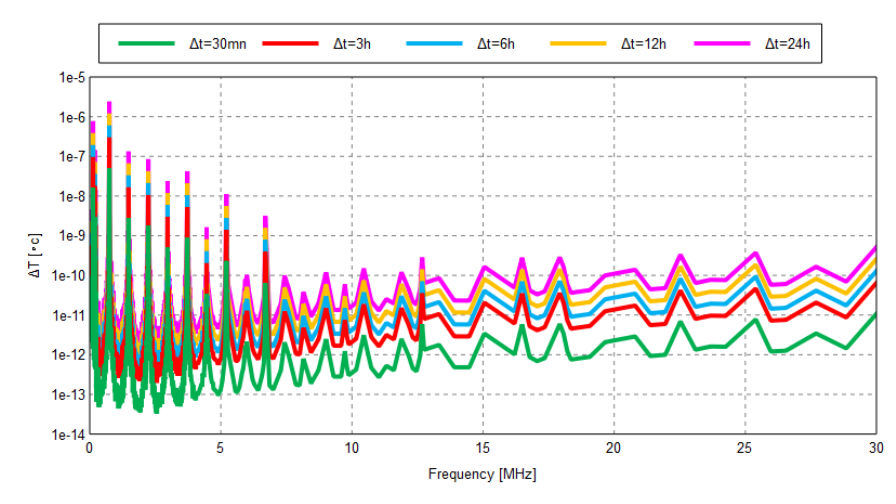


Figure 8: Tissue Temperature Rise

For the most part, the temperature increases are negligible ($\Delta T < 10^{-5}$ °C). However, the temperature rise is greater for small frequencies than for large ones. The penetration depth of the radiation in the tissues explains this, as it is inversely proportional to the frequency.

4. Conclusion

The exposure of a biological entity (human being) to electromagnetic radiation is inevitably accompanied by a biological effect. ICNIRP assesses the impact of exposure to electromagnetic radiation in the PLC frequency band (1-30Mhz) through the SAR. This assessment is complicate as it is almost-impossible to perform SAR measurements on human being "in vivo". This work not only made it possible to generate an expression of the SAR according to the distributed current along the PLC lines but also and above all made it possible to have a simplified expression base of Biot-Savart law. The negligible nature of the health effects due to even prolonged exposure ($\Delta T > 12$ hours) to the radiation from an Outdoor-PLC line (distribution grid) has also been proved. As the intensity of the radiated field decreases drastically with the distance, it is very likely that the radiation from the Indoor-PLC (domestic grid) is probably harmful to health (human).

Acknowledgments

We would like to thank Mr. Salissou Simon, Dr. Mossi and Pr. Madougou of L3EA2I-laboratory for their invaluable support for this work. Their vision and expertise were capital in shaping the direction of this project.

References

- Abatcha, A. K. L., Abdourahimoun, D., Boukar, M., & Madougou, S. (2023). Improvement of the Destructive Interference Method in the Mitigation of PLC Radiation of Imbalanced Impedance Electrical Networks. *American Journal of Energy Engineering*, 11(2), 52–60.
- Alihodzic, A., Mujezinovic, A., Turajlic, E., & Dedovic, M. M. (2022). Determination of Electric and Magnetic Field Calculation Uncertainty in the Vicinity of Overhead Transmission Lines. *Journal of Microwaves, Optoelectronics and Electromagnetic Applications*, 21, 392–413.
- Askari, S., Bastany, Z., Dumont, G., & Shadgan, B. (2023). Active noise cancelling in near-infrared spectroscopy. In B. Shadgan & A. H. Gandjbakhche (Eds.), *Biophotonics in Exercise Science, Sports Medicine, Health Monitoring Technologies, and Wearables IV* (p. 28). SPIE. https://doi.org/10.1117/12.2664609
- CALCUL DU CHAMP MAGNÉTIQUE RAYONNÉ PAR DEUX FILS RECTILIGNES PARALLÈLES PARCOURUS PAR UN COURANT ELECTRIQUE. (n.d.). https://robindestoits-midipy.org
- Determining the peak spatial-average specific absorption rate (SAR) in the human body from wireless communications devices, 30 MHz to 6 GHz Part 3: Specific requirements for using the finite difference time domain (FDTD) method for SAR calculations of mobile phones. (2017). *IEC/IEEE 62704-3:2017*, 1–76. https://doi.org/10.1109/IEEESTD .2017.8089724

- Effect of electromagnetic waves on human reproduction—PubMed. (n.d.). Retrieved May 24, 2023, from https://pubmed.ncbi.nlm.nih.gov/28378967/
- Frère, J. (2017). Caractérisation numérique de l'exposition électromagnétique des personnes en bandes HF et VHF [These de doctorat, Rennes 1]. https://www.theses.fr/2017REN1S027
- ICNIRP | Publications. (n.d.). Retrieved May 24, 2023, from https://www.icnirp.org/en/publications/index.html
- International Commission on Non-Ionizing Radiation Protection. (2022). A Description of ICNIRP'S Independent, Best Practice System of Guidance on the Protection of People and the Environment from Exposure to Non-Ionizing Radiation. *Health Physics*, 122(5), 625–628. https://doi.org/10.1097/HP.0000000000001561
- KONLACK, T. B. C., & TCHUIDJAN, R. (2011, September 1). *Analyse de l'impact des ondes électromagnétiques sur l'homme* [Text]. http://www.afriquescience.info; AUF Agence universitaire de la Francophonie. http://www.afriquescience.info/document.php?id=2188
- Park, K. S. (2023). Biological Effects of Electricity and Electromagnetic Field. In *Humans and Electricity: Understanding Body Electricity and Applications* (pp. 377–400). Springer.
- (PDF) Analysis of Variational Formulations and Low-regularity Solutions for Time-harmonic Electromagnetic Problems in Complex Anisotropic Media. (n.d.). Retrieved May 24, 2023, from https://www.researchgate.net/publication/351337610 Analysis of Variational Form ulations and Low-regularity Solutions for Time-harmonic Electromagnetic Proble ms in Complex Anisotropic Media
- Peng, W., Zhang, W., & An, B. (2020). Radiation Measurement and Analysis of Power Line Communication System for Power Meter Reading. *IEEE Access*, 8, 40989–40999. https://doi.org/10.1109/ACCESS.2020.2976520
- Pola, M. (2023). *Body-Coupled Communication for Microscale Implants In Human Brain* [PhD Thesis]. Politecnico di Torino.
- Poljak, D., Galić, M., & Pajewski, L. (2019). Analytical Calculation of Integral Measures for Quantifying Human Exposure to HF Signals with Continuous Spectra. 2019 23rd International Conference on Applied Electromagnetics and Communications (ICECOM), 1–4.
- Razek, A. (2023). Assessment and Categorization of Biological Effects and Atypical Symptoms Owing to Exposure to RF Fields from Wireless Energy Devices. *Applied Sciences*, 13(3), 1265.
- Vaverka, F., Smetana, M., Gombarska, D., & Psenakova, Z. (2023). Investigation of Microwave Electromagnetic Fields in Open and Shielded Areas and Their Possible Effects on Biological Structure. *Sensors*, 23(4), Article 4. https://doi.org/10.3390/s23042351
- Zagar, T., Valic, B., Kotnik, T., Korat, S., Tomsic, S., Zadnik, V., & Gajsek, P. (2023). Estimating exposure to extremely low frequency magnetic fields near high-voltage power lines and assessment of possible increased cancer risk among Slovenian children and adolescents. *Radiology and Oncology*.